24. M. L. Kaiser and M. D. Desch, *ibid.* 7, 389 (1980).
25. G. Daigne and Y. Leblanc, *J. Geophys. Res.* **91**, 7961 (1986).
26. T. W. Hill, A. J. Dessler, C. K. Goertz, in *Physics of the Jovian Magnetosphere*, A. J. Dessler, Ed. (Cambridge Univ. Press, New York, 1983), p. 353.
27. J. K. Alexander, M. D. Desch, M. L Kaiser, J. R. Thieman, *J. Geophys. Res.* **84**, 5167 (1979).
28. H. P. Ladreiter and Y. Leblanc, *Ann. Geophys.* **8**, 477 (1990).
29. J. L. Green and D A. Gurnett, *Geophys Res. Lett.* **7**, 65 (1980).
30. H. P. Ladreiter and Y. Leblanc, *J. Geophys. Res.* **95**, 6423 (1990).
31. ———, *ibid.* **96**, 21207 (1991).
32. M. D. Desch and M. L. Kaiser, *ibid.* **85**, 4248 (1980).
33. Y. Leblanc and G. Daigne, *ibid.* **90**, 12073 (1985).
34. A. Lecacheux *et al.*, *Geophys. Res. Lett.* **19**, 1307 (1992).

35. We thank R. F. Benson for review of this paper and helpful suggestions and A. Meyer and A. Morane for help with data analysis. The French contribution was financed by the Centre National d'Etudes Spatiales. The French laboratories are associated with the CNRS and are partially funded by this organization via the Institut National des Sciences de l'Univers.

1 June 1992; accepted 31 July 1992

Ulysses Radio Occultation Observations of the Io Plasma Torus During the Jupiter Encounter

M. K. Bird, S. W. Asmar, J. P. Brenkle, P. Edenhofer, O. Funke, M. Pätzold, H. Volland

Radio signals from Ulysses were used to probe the Io plasma torus (IPT) shortly after the spacecraft's closest approach to Jupiter. The frequencies of the two downlinks at S-band (2.3 gigahertz) and X-band (8.4 gigahertz) were recorded, differenced, and integrated in order to derive the columnar electron density of the IPT. The measurements agree qualitatively with contemporary models of the IPT based on Voyager data, but significant differences are apparent as well. The overall level of the IPT electron density is approximately the same as the prediction, implying that the amount of gas (or plasma) injected from Io is similar to that observed during the Voyager era. On the other hand, the IPT seems to be less extended out of the centrifugal equator, implying a smaller plasma temperature than predicted.

The Ulysses spacecraft was occulted by the IPT during its Jupiter encounter on 8 February 1992. The Ulysses dual-frequency radio subsystem used by the Ulysses Solar Corona Experiment (SCE), which was primarily intended for coronal radio sounding investigations and was used during the solar conjunction from July to September 1991 (*1*), was utilized to measure the electron content (column density) of the IPT. The IPT during the Ulysses flyby at Jupiter was found to be slightly higher in peak electron density but slightly lower in mean electron content than predicted by the Voyager-based models. The unique Ulysses occultation geometry was favorable for discriminating between contributions from the sections of the IPT in front of and behind Jupiter, respectively. Initial analysis of the electron content profile indicates that these two contributions are quite different, implying longitudinal asymmetry of the IPT.

The first two spacecraft to fly behind the IPT, Pioneer 10 and Pioneer 11, transmitted only a single S-band downlink. The Doppler shifts of this radio signal caused by the occultation of the IPT are now known to be ≈10 mHz, a value too small to be easily distinguished from other nondispersive perturbations in frequency. Dual-frequency occultations of the IPT occurred during the Jupiter flybys of Voyager 1 and Voyager 2 (5 March and 9 July 1979, respectively). A clear signature of the IPT was obtained at the Voyager 1 flyby (*2*). After corrections for the terrestrial ionosphere had been removed, a peak electron content of some 60 hexems (*3*) was attributed to the IPT (*4*). A more comprehensive analysis of the data (*5*), undertaken with the goal of deriving a more precise mass determination of the Galilean moons, revealed the IPT on the ingress and egress legs of both Voyager trajectories. The IPT electron content measured during the Voyager 2 flyby has not been analyzed in detail (*6*).

It is known that the IPT plane of symmetry is the "centrifugal equator," a plane lying between the rotational equator and the magnetic equator (*7–9*). For this work, it was assumed that the centrifugal equator was tilted by 6.5° with respect to the Jovian rotational equator. This is $2/3\alpha$, where $\alpha = 9.8° \pm 0.3°$ is the dipole tilt angle (*9*). Because the plasma is forced to corotate with the Jovian magnetic field, the IPT wobbles synchronously about Jupiter with the planet's rotation. In order to more effectively display the relation of the IPT to the Ulysses spacecraft and its radio ray path to Earth, Fig. 1 shows three orthogonal views of the Jupiter flyby geometry near the time of Jupiter closest approach (JCA) in a nonrotating "centrifugal" coordinate system. The IPT is stationary in this reference frame.

The z axis of Fig. 1 is perpendicular to the centrifugal equatorial plane. With $\hat{z}$ a unit vector along the z axis, the y axis is chosen perpendicular to the z axis and perpendicular to the Jupiter-Earth vector $\mathbf{r}_{JE}$, such that $\hat{y}$ is given by $\hat{z} \times \mathbf{r}_{JE}/r_{JE}$. The remaining x axis points such that the x, y, and z axes form an orthogonal triad with origin at Jupiter's center. The stylized IPT in Fig. 1 is roughly defined by the electron density contour of $N_e = 1000$ electrons per cubic centimeter. For simplicity, it is taken here to be a symmetric ring, centered on Jupiter, with maximum plasma density at a Jovian distance of 5.5 Jovian radii (R_J). The cross section of the IPT was taken to be elliptical; the radial thickness $d_\rho = 2\ R_J$ and the latitudinal thickness $d_z = 1\ R_J$. The ray paths to Earth are all parallel to the x–z plane, but they change slope in this coordinate system because of the above mentioned wobble (seen best in Fig. 1B). An isometric view of the IPT occultation in this coordinate system from a vantage point above the centrifugal equator may be found in the SCE instrument description (*1*).

The timing of the flyby was such that the ray path first penetrated the IPT in front of Jupiter and then the section closer to Ulysses in back of Jupiter. This situation was not fortuitous. Various mission restrictions were imposed on the Ulysses flyby trajectory at Jupiter in order to assure safe passage of the spacecraft and an optimum postencounter heliocentric trajectory. These restrictions precluded a radio occultation by Jupiter itself. It was also impossible to design a flyby through the IPT density maximum that would still comply with the safety requirement that the Ulysses perijove be greater than 6 R_J. An occultation of the spacecraft by the IPT, however, could "hardly be avoided." Another requirement stipulated that the energetic particle radiation fluence on the Ulysses spacecraft be a minimum. This was accomplished by minimizing the travel time through the IPT, that is, by choosing the encounter time such that the motion of the IPT was opposite to that of the spacecraft. Ulysses thus flew quickly through the Jovian centrifugal equator, just grazing the outer edge of the IPT. The total time spent in the IPT sector behind Jupiter, for both in situ and radio sounding measurements, was only

M. K. Bird, O. Funke, H. Volland, Radioastronomisches Institut, Universität Bonn, 5300 Bonn, Germany.
S. W. Asmar and J. P. Brenkle, Jet Propulsion Laboratory, California Institute of Technology, Pasadena, CA 91109.
P. Edenhofer, Institut für Hochfrequenztechnik, Universität Bochum, 4630 Bochum, Germany.
M. Patzold, Deutsche Forschungsanstalt für Luft- und Raumfahrt, 8031 Oberpfaffenhofen, Germany.

about 1 hour. The frontside IPT, on the other hand, was moving south in the same direction as Ulysses during the occultation and could be detected in the radio occultation data for about 5.5 hours.

Another view of the Ulysses trajectory in the centrifugal coordinate system, superimposed on a contour plot of the IPT electron density distribution according to a model from Bagenal (*10*), is presented in Fig. 2. The radio ray paths assume an unusual form in Fig. 2, moving left from Ulysses to a minimum value of ρ, where they reverse and continue on to Earth, exiting at the right. The ray path segment from the turning point to Ulysses (Earth) passes through space behind (in front of) Jupiter. For example, the ray path denoted for the JCA + 2 hours misses the IPT behind Jupiter but is beginning to traverse the central region of the IPT in front of Jupiter. The minimum offset of the Ulysses radio ray path from Jupiter occurred at 15:12 universal time (UT), approximately 2.5 hours after JCA.

The IPT occultation occurred for the most part in the interval from JCA + 2 hours to JCA + 7.5 hours and was covered in its entirety by the 70-m National Aeronautics and Space Administration Deep Space Network (DSN) station DSS 43 at Tidbinbilla, Australia. Dual-frequency Doppler was recorded at a rate of 1 sample per second. Simultaneous observations of both downlinks were made at the 34-m station DSS 42 at the same DSN complex, but at the reduced sample rate of 1 min^{-1}. Virtually identical data were obtained until problems with the recording system at DSS 43 necessitated switching the high sample rate over to DSS 42. Overlap coverage was provided by the preceding station DSS 14 at Goldstone, California (until the end of Ulysses track at time $t \simeq$ JCA + 2 hours), as well as by the succeeding station DSS 63 at Madrid, Spain (Ulysses track start at $t \simeq$ JCA + 7.5 hours).

One significant geometrical advantage that Ulysses had over Voyager 1 and Voyager 2 was that the Jupiter flyby occurred close to solar opposition. The sun-Earth-probe (SEP) angle was 157°. This meant that possible disturbances due to fluctuations in electron content from non-Jovian sources, namely, the interplanetary medium (IPM) and the terrestrial ionosphere, would be greatly reduced. Variations in the electron content in the IPM are reduced at opposition not only because the interplanetary ray path is shorter and has a larger mean distance from the sun, but also because the view direction is close to the solar wind velocity vector. Changes in interplanetary electron density are therefore convected along the signal ray path rather than through it.

The local time of JCA at DSS 43 was 22:38 hours, so that the IPT occultation took place during nighttime at the ground station. The electron content of the ionosphere over the Australian DSN complex in the direction of Ulysses can be compensated with the use of a model developed at the Jet Propulsion Laboratory for interplanetary navigation (*11*). Application of this ionospheric calibration is a prerequisite for deriving the changes in electron content due to extraterrestrial plasmas. The ionospheric electron content along the Ulysses line of sight at all DSN complexes on the day of the Jupiter encounter is shown in Fig. 3. The time scale of ionospheric variations is typically longer than the 5.5-hour duration of the IPT occultation. Nevertheless, a total excursion of ~40 hexems could be attributed to the terrestrial ionosphere at DSS 43 during the IPT occultation (see Fig. 3). The diurnal variation of the terrestrial ionosphere attained its minimum in electron content at about the same time that the IPT reached its maximum. Even though a significant ionospheric variation is present, large-amplitude ionospheric fluctuations that could be mistaken for the IPT can be excluded.

In order to measure small changes in the electron content along the Ulysses signal ray path, the preferred radio subsystem configuration is S-band uplink, and S/X-band (dual-frequency) downlink, both downlinks being phase coherent with the uplink. This is the standard radio subsystem configuration for the SCE investigation. Although it was thought to be conceivably possible to extract the IPT signature using only the primary telemetry link at X-band, an esti-

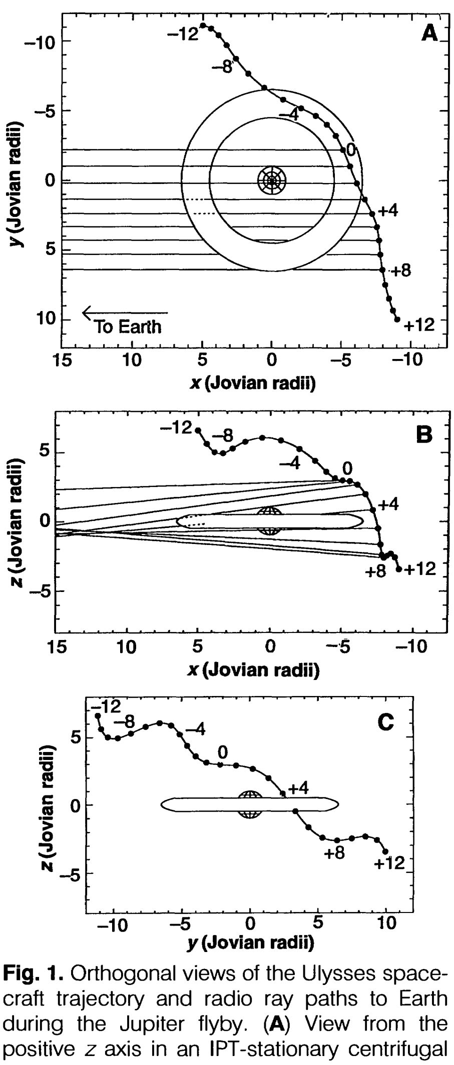

Fig. 1. Orthogonal views of the Ulysses spacecraft trajectory and radio ray paths to Earth during the Jupiter flyby. (**A**) View from the positive *z* axis in an IPT-stationary centrifugal coordinate system. (**B**) View from the positive *y* axis. (**C**) View from the positive *x* axis. The projected position of Ulysses along its trajectory is given by the dots that indicate the time (in hours) with respect to the time of JCA, 12:38 UT, ground received time. The radio ray paths from Ulysses to Earth, shown for each hour beginning at JCA and ending at JCA + 8 hours, are drawn as follows: in front of the IPT, solid lines; behind the IPT, not drawn; inside the IPT, dashed lines.

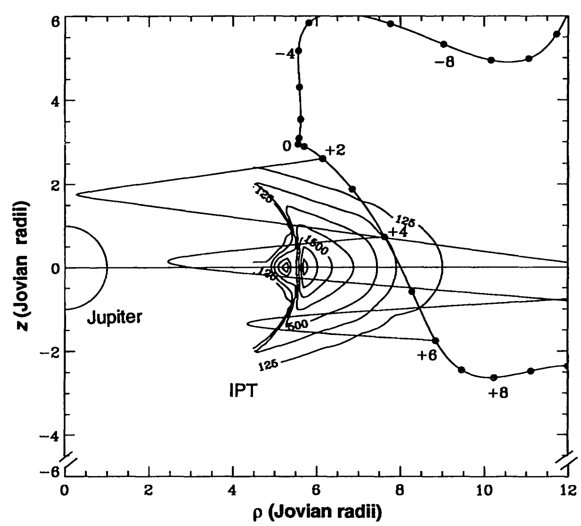

Fig. 2. Ulysses trajectory in the centrifugal coordinate system. The position of Ulysses is plotted as a function of distance from the centrifugal equator (*z*) and distance from the centrifugal *z* axis (ρ) in this rotating meridian plane projection. The numbers near the solid dots along the trajectory refer to time in hours with respect to JCA. Projections of the radio ray path from Ulysses to Earth in this plane are indicated for the three times +2, +4, and +6 hours. Contours of equal electron density (electrons per cubic centimeter) in the IPT according to the numerical model of Bagenal (*10*) are superimposed.

mated 100-fold increase in sensitivity could be gained with the use of the dual-frequency technique (*12*). One drawback to dual-frequency operations, however, is the higher power consumption (the S-band transmitter requires 35 W of dc power). In fact, the technical feasibility of the IPT occultation experiment was in doubt as Ulysses approached Jupiter because it was unclear whether the predicted available power would suffice for dual-frequency operations during the flyby.

Radio-sounding techniques for remote sensing of ionized media along the propagation path between Ulysses and ground station can be applied to the solar corona (*13*), but also virtually to any other planetary plasma (*14*). The specific approach used to extract the electron content of the IPT is outlined here for completeness.

For coherent operation of the Ulysses radio subsystem, the received downlink frequency f_d can be expressed as:

$$f_d = kf_u + k\delta f_u - 2kf_u\frac{\dot{s}_0}{c} - 2kf_u\frac{\delta\dot{s}_0}{c} + \frac{40.3}{ckf_u}(k^2\dot{I}_u + \dot{I}_d) \qquad (1)$$

where k is the transponder turnaround ratio, which is equal to 240/221 for S-band up/S-band down; and 880/221 for S-band up/X-band down; f_u is the uplink frequency (2111.6 MHz for Ulysses); δf_u is a small deviation from nominal uplink frequency due to oscillator instability; $\dot{s}_0$ is the predicted topocentric radial velocity from the computed trajectory; $\delta\dot{s}_0$ is the residual topocentric radial velocity not included in $\dot{s}_0$; $\dot{I}_{u,d}$ is the time derivative of the total electron content along the uplink (u) or downlink (d), respectively; and c is the speed of light. The X-band to S-band downlink frequency ratio is $f_x/f_s = k_x/k_s = 11/3$.

The first and third terms of Eq. 1 are known and are subtracted from the received frequency to obtain a "frequency residual" containing contributions from such sources as oscillator instabilities, intervening plasma, and trajectory errors. It is often convenient to integrate the frequency residuals to obtain the residual phase, a quantity directly proportional to changes in the electron content along the signal ray path. If both S- and X-band downlinks are available, one obtains two observable phases m_s and m_x:

$$m_s = k_s\delta f_u t - 2k_s f_u\frac{\rho}{c} + \frac{40.3}{ck_s f_u}(k_s^2 I_u + I_d) \qquad (2)$$

$$m_x = k_x\delta f_u t - 2k_x f_u\frac{\rho}{c} + \frac{40.3}{ck_x f_u}(k_x^2 I_u + I_d) \qquad (3)$$

with

$$\rho = \int \delta\dot{s}_0 dt \text{ and } I_{u,d} = \int N_e ds_{u,d} \qquad (4)$$

where N_e is the electron density, integrated to yield the columnar electron content $I_{u,d}$ along the uplink (u) and downlink (d) ray paths, respectively. The frequency dependence of Eqs. 2 and 3 may be exploited to isolate the phase changes due to plasma along the downlink by computing the linear combination:

$$\delta m_s = m_s - \frac{k_x}{k_s}m_x = \frac{40.3}{ck_s f_u}\left(1 - \frac{k_s^2}{k_x^2}\right)I_d \qquad (5)$$

The differential phase δm_s is governed exclusively by the plasma. All nondispersive effects on the Doppler shift due to oscillator drift or trajectory errors are eliminated. The differential phase (Eq. 5) is expressed in cycles at S-band for all other parameters in SI units. If the electron content is expressed in "hexems," then Eq. 5 can be written as:

$$I_d \text{ (hexems)} = 1.843\delta m_s \text{ (cycles at S-band)} \qquad (6)$$

The sensitivity of the S/X-band Doppler measurements with Ulysses has been estimated to be $\sim\pm10°$ at S-band (*1*), which from Eq. 6 translates to ±0.05 hexem. This is more than a factor of 1000 less than the actually measured peak electron content from the IPT.

The differential frequency measurements recorded at the Australian DSN complex during encounter and the subsequently derived electron content of the IPT are shown in Fig. 4, A and B, respectively. The data are presented here as a function of ground received time rather than the conventional spacecraft event time used by the Ulysses in situ investigations. In order to avoid misunderstandings in timing, most references to features in the observations and other events will be given in terms of their relation to JCA.

We calculated simulated values of electron content and plotted them in Fig. 4 for the IPT models of Bagenal (*10*) and Divine-Garrett (*15*) by integrating along the signal ray paths. Considering the limited range of the in situ data used for the models, it is remarkable that they produce such an accurate prediction for the IPT electron content profile during the Ulysses flyby.

The Ulysses measurements displayed in Fig. 4 were processed as follows: (i) The differential frequency residuals $\delta f_s - (3/11)\,\delta f_x$ were recorded directly. (ii) The resultant differential frequency residuals were corrected for the known spin bias (*16*) by removal of a constant offset. (iii) The spin-compensated differential frequency residuals were integrated, beginning at 12:00 UT, to obtain the change in total electron content from that starting point. (iv) The contribution to the total electron content from Earth's ionosphere (*11*) was subtracted

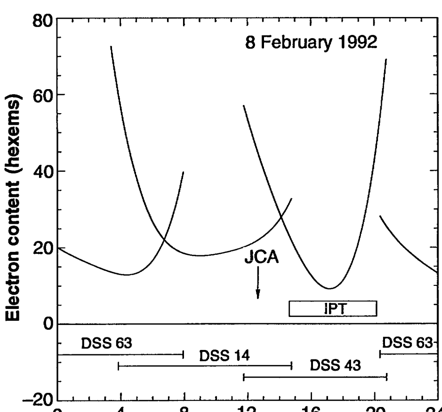

Fig. 3. Ionospheric electron content calibrations. Faraday rotation measurements from geostationary satellites are used to compute ionospheric calibrations for deep space tracking applications (*11*). The four individual curves show the calibrated ionospheric electron content (in hexems) along the Ulysses ray path to all DSN stations on the day of the Jupiter encounter. The actual times of each Ulysses tracking pass are indicated along the bottom of the plot.

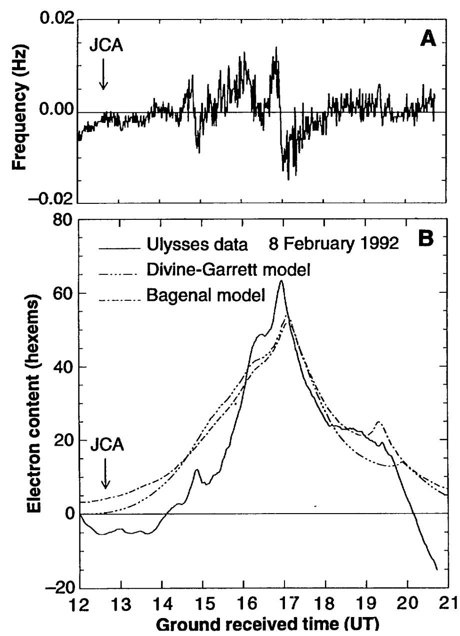

Fig. 4. IPT electron content during the Ulysses Jupiter flyby. (**A**) Differential frequency measurements after removal of spin bias (*16*). (**B**) Differential phase, the integral of (A), after removal of contributions from Earth's ionosphere and the interplanetary medium. The observations are plotted at 1-min intervals, each point being an average over 60 measurements taken at a sample rate of 1 s^{-1}. The data from DSS 43 and DSS 42 were spliced together at 18:30 UT owing to Doppler recording anomalies at DSS 43. Solid curve: actual measurements. Dash-dotted curve: simulated IPT electron content using the Bagenal model (*10*) and integrating along the radio ray paths as indicated in Fig. 2. Dash-triple dotted curve: Simulated IPT electron content using the Divine-Garrett model (*15*).

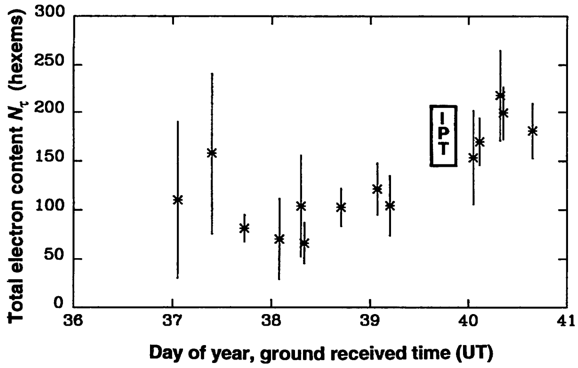

Fig. 5. Electron content between Ulysses and ground station obtained from dual-frequency ranging observations before and after JCA. Ranging during the IPT occultation was suppressed, primarily to improve the signal-to-noise ratio of the S-band carrier signal. The interplanetary medium during the Jupiter encounter increased from ~100 to ~150 hexems during the IPT occultation. This linear increase correlates satisfactorily with the background trend observed in the Doppler measurements and was removed in order to obtain the IPT signature displayed in Fig. 4.

to obtain the electron content from extraterrestrial sources alone. (v) In order to remove long-term changes in the background electron content from the interplanetary medium, we detrended the resultant curve by removing a linear background contribution. Only pre- and postoccultation time segments were used to establish the background baseline.

Figure 5 shows the dual-frequency ranging measurements between Ulysses and Earth during the days around Jupiter encounter (day of year 39 corresponds to 8 February). The time of the IPT occultation and the estimated peak IPT electron content (60 hexems) are indicated in Fig. 5 by the box labeled "IPT." It was known that ranging measurements would not be sensitive enough to measure plasma variations of the IPT; the typical error bars in Fig. 5 are of the order of the peak IPT, electron content. These ranging data, however, do give a rough measure of the absolute electron content in the IPM, rather than just the changes in electron content. The values lie between 100 and 150 hexems, quite typical for a propagation path length of 4.48 astronomical units (AU) near opposition. There is an apparent upward trend in electron content on encounter day that was removed in step (v) to produce the final IPT electron content profile of Fig. 4.

Some obvious differences between the radio occultation measurements and the model simulations may be noted. Whereas the observed IPT electron content profile attains a peak of 65 hexems at 16:57 UT (JCA + 4^h 19^m), the models predict that an absolute maximum of ~50 hexems should be seen about 10 min later. Although two peaks are clearly distinguished in the measurements, they are not well separated in the model simulations. Finally, the rise in IPT electron content occurs much more steeply than the predictions. The inferred smaller extent of the IPT out of the centrifugal equator would imply that the (ion) temperature is less than predicted.

The relative maximum observed at 16:29 UT (JCA + 3^h 51^m) is attributed to the Ulysses ray path passing through the IPT in front of Jupiter. The IPT sector probed at this time was centered at magnetic longitude $\lambda_{III} = 50°$. The position of this sector at this time was only about 2 R_J in the direction of corotation from Io, the proven source of the plasma in the IPT (*7*, *9*). The absolute maximum recorded 30 min later occurs when the center of the IPT behind Jupiter is probed by the ray path at magnetic longitudes near $\lambda_{III} = 310°$. The timing of this maximum correlates very well with in situ measurements from the Unified Radio and Plasma Wave (URAP) investigation on Ulysses (*17*). The peak electron density recorded by URAP along the Ulysses trajectory was slightly higher than the model predictions, consistent with the electron content observations reported here.

The slight negative excursion of the measurements for the first 2 hours of data in Fig. 4 reflects the changes in electron content not related to the IPT, starting at 12:00 UT. The magnitude of this fluctuation (~5 hexems) is estimated to be of the order of the systematic error associated with the profile in Fig. 4. The small relative maximum observed at 14:52 UT is most probably of Jovian origin. The possibility of its being an ionospheric disturbance is excluded because the same feature was observed simultaneously at the DSN stations in Australia and California. The data also display a plateau-like region of nearly constant electron content (≃20 hexems) starting at about 18:00 UT and lasting for about 90 min. The enhanced IPT electron content in this interval is attributed to the geometry of the occultation, in particular, to the proximity of the Ulysses ray path to the west ansa of the IPT. The Ulysses radio ray path remained almost stationary in z just below the IPT in front of Jupiter (Fig. 1), passing under the ansa at approximately 19:30 UT (JCA + 7^h). A ray path passing through the ansa is most favorable for producing a maximum in the IPT electron content profile.

We made certain modifications to the Bagenal model in an attempt to find what parametric changes would lead to a better representation of the radio occultation data. Variable parameters introduced were the following: (i) the z coordinate of maximum electron density (affecting the timing of the peak electron content), (ii) the overall level of electron density (affecting the height of the electron content peak), and (iii) the scale height of the electron density falloff away from the centrifugal equator (affecting the slope of the electron content profiles during ingress and egress).

The principal finding of this parametric study was that a satisfactory fit to the observed profile could not be generated with an azimuthally symmetric IPT. Initial results indicate that significantly different parameter sets may be necessary for the IPT on opposite sides of Jupiter. One possible explanation for the difference would be a density maximum arising from a magnetic anomaly as proposed by Dessler and Hill (*18*). It is also consistent with reported longitudinal asymmetries in ground-based line emission observations of ionized sulfur (*19*). A quantitative description of these simulations with modified models of the IPT will be presented in subsequent publications.

The Ulysses IPT occultation experiment has verified the accessibility of the IPT to radio science techniques usually applied to planetary atmospheres and ionospheres. It is hoped that these investigations can be continued with the Galileo spacecraft at its frequent IPT occultation opportunities during the Jovian orbital tour beginning in late 1995 (*20*).

REFERENCES AND NOTES

1. M. K. Bird *et al.*, *Astron. Astrophys. Supp. Ser.* **92**, 425 (1992); M. Pätzold *et al.*, in *Solar Wind Seven*, E. Marsch and R. Schwenn, Eds. (Pergamon, Oxford, 1992), pp. 237–240.
2. V. R. Eshleman *et al.*, *Science* **206**, 959 (1979); *ibid.* **204**, 976 (1979).
3. The "hexem" (10^{16} electrons per square meter) is a convenient unit for columnar electron density.
4. G. S. Levy, D. W. Green, H. N. Royden, G. E. Wood, G. L. Tyler, *J. Geophys. Res.* **86**, 8467 (1981).
5. J. K. Campbell and S. P. Synnott, *Astron. J.* **90**, 364 (1985).
6. J. K. Campbell and R. F. Sunseri, *Eos* **66**, 947 (1985); J. K. Campbell, unpublished memorandum (Jet Propulsion Laboratory, Pasadena, CA).
7. J. W. Belcher, in *Physics of the Jovian Magnetosphere*, A. J. Dessler, Ed. (Cambridge Univ. Press, Cambridge, 1983), chap. 3; R. A. Brown, C. B. Pitcher, D. F. Strobel, *ibid.*, chap. 6.
8. T. W. Hill, A. J. Dessler, F. C. Michel, *Geophys. Res. Lett.* **1**, 3 (1974).
9. T. W. Hill, A. J. Dessler, C. K. Goertz, in *Physics of the Jovian Magnetosphere*, A. J. Dessler, Ed. (Cambridge Univ. Press, Cambridge, 1983), chap. 10; A. J. Dessler, *ibid.*, appendix B.
10. F. Bagenal, R. L. McNutt, Jr., J. W. Belcher, H. S. Bridge, J. D. Sullivan, *J. Geophys. Res.* **90**, 1755 (1985); F. Bagenal and J. D. Sullivan, *ibid.* **86**, 8447 (1981); F. Bagenal and J. D. Sullivan, *Geophys. Res. Lett.* **7**, 41 (1980).
11. "DSN tracking system interfaces: Media calibration data interface" (Jet Propulsion Laboratory Internal Document 820-13, Rev. A, Pasadena, CA, 1985).
12. A much more difficult measurement could still

have been attempted in the event that only the X-band downlink, coherent with the S-band uplink, were available. In this case the IPT signature would be imposed on the S-band uplink and then transponded to ground at the standard DSN frequency turnaround ratio of 880/221. If we compare the X-band received frequency with an orbit-corrected frequency prediction, it is still technically possible to extract the subtle phase shift expected from the IPT. For all practical purposes, however, the Doppler shifts expected from the gravitational perturbations of the Jovian moons and higher moments of Jupiter's gravity field would all tend to mask the desired signal.

13. M. K. Bird and P. Edenhofer, in *Physics of the Inner Heliosphere*, R. Schwenn and E. Marsch, Eds. (Springer-Verlag, Heidelberg, 1990), vol. 1, chap. 2; M. K. Bird, *Space Sci. Rev.* **33**, 99 (1982).
14. G. L. Tyler, *Proc. IEEE* **75**, 1404 (1987).
15. N. Divine and H. B. Garrett, *J. Geophys. Res.* **88**, 6889 (1983).
16. It can be shown that the differential frequency residual will have a small bias due to the spin of the spacecraft. For the Ulysses S/X-band system, the bias from the nominal 5-rpm spacecraft rotation f_{spin} will amount to $f_{\mathrm{bias}} = 8f_{\mathrm{spin}}/11$. The attitude control data during the IPT occultation indicate that the actual spin period was 12.039 s, so that $f_{\mathrm{bias}} \simeq 0.0604$ Hz.
17. R. G. Stone *et al.*, *Science*, **257**, 1524 (1992).
18. A. J. Dessler and T. W. Hill, *Geophys. Res. Lett.* **2**, 567 (1975).
19. L. Trafton, *Icarus* **42**, 111 (1980); J. T. Trauger, G. Münch, F. L. Roesler, *Astrophys. J.* **236**, 1035 (1980); C. B. Pilcher and J. S. Morgan, *ibid.* **238**, 375 (1980). A recent review of optical observations of the IPT and its associated neutral clouds has been written by N. Thomas, *Surv. Geophys.*, in press.
20. As described by H. T. Howard *et al.* [*Space Sci. Rev.* **60**, 565 (1992)], the geometrical constellations assumed by the Galileo spacecraft during its Jupiter tour beginning in late 1995 will provide many opportunities to repeat this occultation experiment. The harsh radiation environment of the IPT will restrict in situ investigation of the IPT with Galileo to the inbound and outbound passes surrounding the Jupiter orbit insertion. Unfortunately, Galileo will be severely handicapped in its radio science program at Jupiter unless that spacecraft's problematic high gain antenna (HGA) is successfully deployed. Should the HGA remain nonfunctional, the only available downlink will be at S-band from either of two low gain antennas (LGAs). In addition to a loss of some 30 dB going from the HGA to the LGA, it will be very difficult to isolate the effects of plasma variations along the signal's propagation path without exploiting the dispersive Doppler shift from the originally designed phase-coherent downlinks at both S- and X-band.

21. The IPT occultation experiment could not have been performed without the outstanding efforts of the Radio Science Support Team at the Jet Propulsion Laboratory. We acknowledge especially valuable contributions from A. S. Devereaux, P. M. Eshe, R. G. Herrera, T. Horton, and D. D. Morabito. We thank F. Bagenal for supplying us with a hand-tailored IPT model that could be most effectively used in our simulation studies. We appreciate the encouragement for the IPT occultation experiment and the many helpful comments to this initial report provided by A. J. Dessler. Much of the research described in this paper was carried out at the Jet Propulsion Laboratory, California Institute of Technology, under a contract with the National Aeronautics and Space Administration. This paper presents results of a research project partially funded by the Deutsche Agentur für Raumfahrtangelegenheiten GmbH under contract 50 ON 9104, and by the Deutsche Forschungsanstalt für Luft- und Raumfahrt, Institut für Hochfrequenztechnik, NE-HF. The responsibility for the contents of this publication is assumed by the authors.

1 June 1992; accepted 11 August 1992

Plasma Composition in Jupiter's Magnetosphere: Initial Results from the Solar Wind Ion Composition Spectrometer

J. Geiss, G. Gloeckler, H. Balsiger, L. A. Fisk, A. B. Galvin, F. Gliem, D. C. Hamilton, F. M. Ipavich, S. Livi, U. Mall, K. W. Ogilvie, R. von Steiger, B. Wilken

The ion composition in the Jovian environment was investigated with the Solar Wind Ion Composition Spectrometer on board Ulysses. A hot tenuous plasma was observed throughout the outer and middle magnetosphere. In some regions two thermally different components were identified. Oxygen and sulfur ions with several different charge states, from the volcanic satellite Io, make the largest contribution to the mass density of the hot plasma, even at high latitude. Solar wind particles were observed in all regions investigated. Ions from Jupiter's ionosphere were abundant in the middle magnetosphere, particularly in the high-latitude region on the dusk side, which was traversed for the first time.

The interaction of the solar wind with planets, the moon, or comets takes on different forms, and comparative studies of these interactions are an important part of space plasma physics and solar system research. For example, the main energy for magnetospheric processes is believed to be supplied by the solar wind in the case of Earth but by the planet's rotation in the case of Jupiter (*1, 2*). In fact, the Jovian magnetosphere is characterized by significant plasma pressures and strong centrifugal forces resulting from the fast rotation of the planet, its strong magnetic field, and a large abundance of heavy ions from the volcanic satellite Io. With the Solar Wind Ion Composition Spectrometer (SWICS) on board Ulysses, we obtained representative and comprehensive data on the plasma composition in the Jovian magnetosphere, allowing us to study sources and transport of different ion species. This information also enables us to determine the mass loading in the rotating magnetic field of Jupiter, which in turn determines the effect of centrifugal forces on the overall geometry and dynamics of the Jovian magnetosphere. In this report we give a preliminary account of our findings.

The design of SWICS, its capabilities, operational modes, and performance in flight are described in (*3*). The instrument combines energy-per-charge separation by an electrostatic analyzer (0.6 to 60 keV/*e*), acceleration (23 kV), time-of-flight measurement, and determination of total energy with solid-state detectors. For an ion producing a triple coincidence (two time-of-flight and one solid-state detector signals), this technique allows the determination of its mass (M) and charge (*q*) separately so that different ion species can be distinguished even if they have equal *M*/*q* ratios. A double coincidence (time-of-flight only) permits only measurement of the *M*/*q* ratio (*4*). The coincidence methods used suppress background, an important feature in the strong radiation fields of the Jovian magnetosphere (*5*).

SWICS is optimized for solar wind conditions. The collimator accepts ions arriving in a cone of 60° half-width around the spin axis pointing toward Earth. Thus, SWICS covered only a part of the angular distribution of the magnetospheric ions. In particular, it viewed the corotation direction only on the outbound, dusk, high-latitude path.

Figure 1 gives an overview of the ion populations from 0.6 to 60 keV/*e* we encountered in the Jovian environment. The bow-shock crossings are readily recognizable in the SWICS data: the count rates for H^+ and He^{2+} were reduced in the magnetosheath because there, in the high-temperature, low-speed environment, our instrument did not cover the whole energy range and angular distribution of these ions as it does in the highly supersonic solar wind. The multiple entries into and exits out of the magnetosphere were marked by the prompt appearance and disappearance of S and low-charge O ions, as well as by increased background counts caused by penetrating electrons in the individual detectors. For instance, the short excursion back into the magnetosheath (actually, a mixed

J. Geiss, H. Balsiger, U. Mall, R. von Steiger, Physikalisches Institut, Universität Bern, 3012 Bern, Switzerland.
G. Gloeckler, A. B. Galvin, D. C. Hamilton, F. M. Ipavich, Department of Physics, University of Maryland, College Park, MD 20742.
L. A. Fisk, Office of Space Science and Applications, National Aeronautics and Space Administration, Washington, DC 20546.
F. Gliem, Institut für Datenverarbeitende Anlagen, Technische Universitat, 3300 Braunschweig, Germany.
S. Livi and B. Wilken, Max-Planck-Institut fur Aeronomie, 3411 Katlenburg-Lindau, Germany.
K. W. Ogilvie, National Aeronautics and Space Administration, Goddard Space Flight Center, Greenbelt, MD 20770.